

Part E: Nondestructive Testing

Non-destructive Testing

General Concepts

The Southwell Plot

Examples

Some Background

Underlying General Theory

Snap-Through Revisited

Effect of Damping

Range of Prediction

A Box Column

Plates and Shells

Nondestructive Testing

We have seen the often near **linear** relation between the axial load (providing it is less than critical) and square of the effective natural frequency

$$\frac{\omega^2}{\omega_0^2} = 1 - \frac{P}{P_{cr}}. \quad (1)$$

For example, consider a simple cantilever. The fundamental frequencies in bending have the mode shapes

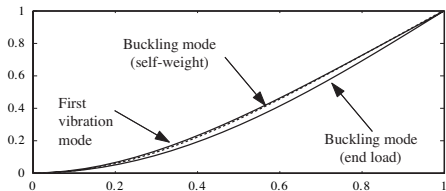
$$W(x) = \cosh\left(\frac{\lambda_i x}{L}\right) - \cos\left(\frac{\lambda_i x}{L}\right) - \sigma_i \left[\sinh\left(\frac{\lambda_i x}{L}\right) - \sin\left(\frac{\lambda_i x}{L}\right) \right] \quad (2)$$

with $\sigma_1 = 0.7341$, $\lambda_1 = 1.8751$ for the lowest mode and corresponding frequency (i.e., $\omega_1 = 3.516\sqrt{EI/(mL^4)}$). The buckling mode for a cantilever with an end load is given by

$$W(x) = 1 - \cos\left(\frac{\pi x}{2L}\right) \quad (3)$$

with a critical load of $P_{cr} = \pi^2 EI/(4L^2)$.

These normalized shapes are plotted below. They are close, but unlike the pinned-pinned (and some sliding boundary conditions) case, they are not equal.



Comparison of vibration and buckling mode shapes for a uniform cantilever.

However, also plotted in this figure (as the dashed line) is the buckling mode shape corresponding to the cantilever subject to self-weight. This is much closer to the fundamental mode of vibration, and in fact, the difference between them is never more than 1%.

The **equivalence** of the vibration and buckling mode shapes results in the linear relation between axial load and frequency, i.e., the extent to which the vibration mode shape is changed by axial loading. Thus we have a frequency(squared) v load relation that is closer to linearity for the vibrations of a cantilever subject to self-weight than an end load. However, even for the end-loaded cantilever case a simple use of ABAQUS shows that when $(P/P_{cr}) = 0.51875$ we obtain a lowest natural frequency of $(\omega/\omega_0)^2 = 0.43804$ compared with an estimate of $(\omega/\omega_0)^2 = 0.41825$ suggested by the linear relation.

Thus, we see the possibility of using dynamics as a means of assessing axial load effects including the prediction of buckling. In static buckling tests it is often unavoidable that specimens are destroyed during the experimental procedure (often the result of plastic deformation during large deflections). The Southwell plot is a related static approach that also exploits a linear extrapolation to predict buckling nondestructively. Correlation studies between dynamic response and stiffness are also used to determine the actual boundary conditions as well. The simplicity of this relation can be used to non-destructively test axially-loaded slender structural elements through monitoring of dynamic response.

The Southwell Plot

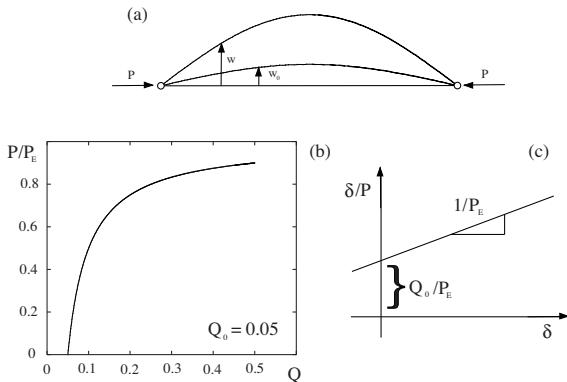
We have seen how a small initial geometric imperfection tended to amplify the lateral deflections of a strut, especially as the buckling load is approached. In an experimental context we would typically measure the lateral deflection **over and above** the initial deflection, which we can call $\delta = w - w_0$. If we assume the initial deflection is in the form of a half-sine wave of amplitude Q_0 , we can plot the amplification effect (assuming small deflections). Thus (at the mid-point of the strut)

$$\delta = \frac{Q_0}{1 - P/P_E} - Q_0 = Q_0 \frac{P/P_E}{1 - P/P_E}. \quad (4)$$

Equation (4) can be arranged in the form

$$\frac{\delta}{P} = \frac{\delta}{P_E} + \frac{Q_0}{P_E}, \quad (5)$$

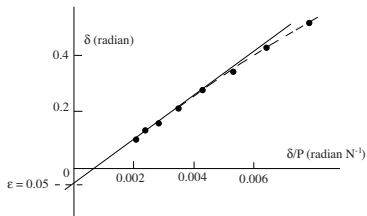
so that if we plot δ/P as a function of δ we get a **straight line** in which the intercept is given by Q_0/P_E and the slope is given by $1/P_E$.



The Southwell plot, (a) strut geometry with an initial imperfection, (b) axial load - lateral deflection relation, (c) Southwell plot.

Southwell recognized the usefulness of this approach in order to determine both the critical load and initial imperfection, and this is shown schematically in part (c).

A Southwell plot based on experimental data is shown below:

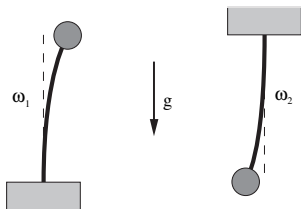


The Southwell plot using experimental data taken from an earlier experimental system (Croll and Walker).

Here, the data suggests a critical load (slope) in the vicinity of 87 N and an imperfection of $\epsilon \approx 0.05$ or about 3 degrees, values not unreasonable when compared with the data (from the link model) presented earlier. Although there are limitations to this approach, the key utility here is that the linear relation allows for **extrapolation**. This provides some motivation for exploring related concepts in the dynamic testing of structures, where vibration testing **in situ** is a well established procedure, e.g, in structural health monitoring.

Examples

The relation between axial load and lateral vibrations and its potential use for non-destructive evaluation purposes goes back to Sommerfeld. He made the simple observation that the fundamental natural frequencies of the two systems shown below were quite different (with $\omega_2 > \omega_1$).



The effect of axial load direction on natural frequencies.

He concluded that the greater the compressive stress, the lower the natural frequency of lateral vibration. With tensile stress, an increase in natural frequency was observed. Furthermore, in the former case it was noted that the frequency dropped to zero as the compressive load approaches its critical value.

We can conduct a simple analysis of this system using the methods developed earlier in this book. Suppose the strut has a length, l , end mass, m , flexural rigidity, EI , and oscillates in gravity, g . Introducing the nondimensional parameter $\alpha = \sqrt{mg/EI}$ it can be readily shown that when the strut has the mass placed at its top, the natural frequency is given by

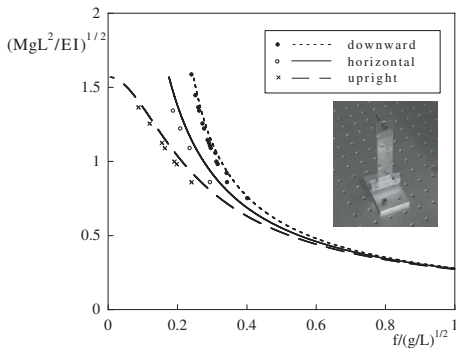
$$\omega = \sqrt{g\alpha/(\tan \alpha l - \alpha l)}, \quad (6)$$

which remains positive until buckling occurs at $m_c = \pi^2 EI/4gl^2$. When the strut is turned upside down (b) the natural frequency becomes

$$\omega = \sqrt{g\alpha/(\alpha l - \tanh \alpha l)}. \quad (7)$$

Thus, suppose we have a mass that corresponds to about the half the critical load, i.e., $m = (\pi^2 EI)/(8gl^2)$, then $\alpha = \pi/(2\sqrt{2}l)$ and the natural frequency of the system in part (a) would be $1.106\sqrt{g/l}$, as opposed to $1.904\sqrt{g/l}$ for the system in part (b). In fact, even a mass that causes buckling in part (a) would result in oscillations of frequency $1.55\sqrt{g/l}$ in the inverted system (part (b)).

It is quite easy to demonstrate this experimentally using a polycarbonate cantilever strip as shown in the inset to figure below.

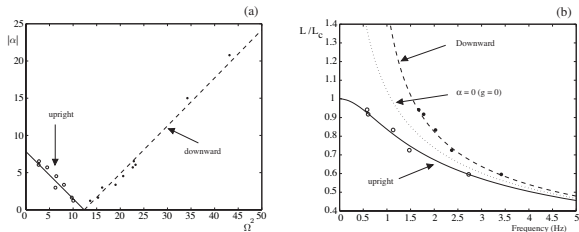


(a) A simple experimental cantilever and its frequency variation with end load for different orientations.

We also note at this point that experiments on cantilevers with self-weight loading are relatively easy to set up. The results from tests using other boundary and loading conditions, e.g., in a testing machine, need more careful interpretation.

As a reference point the typical amount of end mass the strut was able to withstand before appreciably starting to droop to one side was about 27g. The Euler load for a cantilever is $EI\pi^2/(4L^2)$ which gives a value of $m_c = 35\text{g}$, and given the inevitable initial imperfections in the system this magnitude is not unreasonable. Furthermore, when no end mass was added the strut vibrated with a measured natural frequency of a little over 6 Hz (in fact 6.075, 6.2375 and 6.4 in its upright, horizontal and downward orientations). The **theory of continuous elastic beams** gives a fundamental natural frequency for a cantilever of $\omega = 3.52\sqrt{EI/mL^4}$ and with the total mass of the strip measured at $mL = 5.94 \times 10^{-3}$ Kg this corresponds to a predicted frequency of 6.38 Hz.

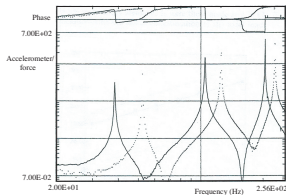
Returning to self-weight loading the 'weight' parameter $|\alpha|$ can also be plotted as a function of frequency squared (part (a) below). In the absence of gravity we would expect the frequency to be proportional to the inverse of the length squared, and this case is shown too. However, in the upright configuration, as the critical length is approached the stiffness is diminished such that the frequency drops to zero at the critical length. If we plot the dimensional frequency versus the length (normalized by the critical length) we get the results shown in part (b). However, not all the data from part (a) are included because of different thicknesses.



The frequencies of a simple but heavy experimental cantilever. The continuous line represents the upright case, the dashed line represents the hanging down orientation. (a) $|\alpha|$ vs. the fundamental frequency squared, (b) alternative plot of the same results.

Thus, we might measure the fundamental natural frequency for a number of different α values (specifically changing the length L) and fitting a straight line to the data we would *predict* buckling in the vicinity of $\alpha \approx 7.8$. Recall that in this plot the "weight" α is a nondimensional parameter given by $\alpha = mgL^3/(EI)$, and hence with mass per unit length of 0.0147 kg/m, cross sectional dimensions of 25.4×0.508 mm and Young's modulus of 2.4 GPa we get the actual length at buckling of about 0.33m. The cantilever that hangs down never buckles as the length increases of course.

If the trend is linear then it also provides the possibility of predicting the elastic buckling not only from, in principle, measurement of the lower natural frequency at two distinct axial loading conditions but even when one or more of these loads are **tensile**.



Frequency content of a prismatic beam showing the shift in resonant frequencies under the application of axial loading (Livingston et al.).

Over this frequency range the lowest three frequencies are quite distinct. The continuous line corresponds to (practically) zero axial loading, with the dotted line showing the shift to higher frequencies when the beam is subject to a tensile axial load (approximately of a similar magnitude to the Euler buckling load with boundary conditions somewhat intermediate between clamped and pinned).

Some Background

Major contributions were made by Massonet, who considered a variety of structural systems from a theoretical standpoint, and Lurie, who showed the utility of this approach including experiments. Even when the mode of vibration and buckling mode are not identical the load-frequency (squared) relation may be almost linear. Lurie used an energy approach to show that an upper limit for the frequency of axially-loaded thin beams resulted in a relation

$$1 \geq \frac{m\omega^2}{EI} \frac{\int_0^l w^2 dx}{\int_0^l \left(\frac{d^2w}{dx^2}\right)^2 dx} + \frac{P}{EI} \frac{\int_0^l \left(\frac{dw}{dx}\right)^2 dx}{\int_0^l \left(\frac{d^2w}{dx^2}\right)^2 dx}. \quad (8)$$

For example, consider a clamped-clamped beam for which we know that $P_{cr} = 4\pi^2 EI/l^2$ and $\omega_n(P = 0) = 22.373\sqrt{EI/(ml^4)}$, and using the buckling mode shape

$$w = A \left[1 - \cos \frac{2\pi x}{l} \right] \quad (9)$$

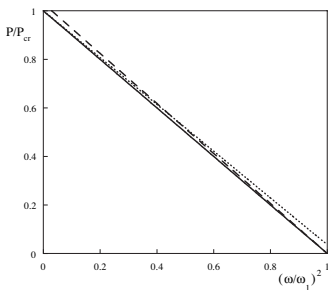
results in an expression

$$1 \geq 0.9635 \left(\frac{\omega}{\omega_n} \right)^2 + \frac{P}{P_{cr}}. \quad (10)$$

Using the lowest mode of vibration results in

$$1 \geq \left(\frac{\omega}{\omega_n} \right)^2 + 0.9704 \frac{P}{P_{cr}}. \quad (11)$$

Equations (10) and (11) are plotted as **inequalities** in the figure below together with the linear relation (equation 1).



Upper and lower bounds of the frequency-load relation for a clamped-clamped beam.

Thus we see the possibility of exploiting the linear relation between the square of the lowest natural frequency and the level of axial loading to extrapolate critical conditions.

Underlying General Theory

We have repeatedly looked at systems with a stiffness that tended to be diminished by the presence of (compressive) axial loading. In terms of potential energy we can write this as

$$V = U(q_i) - \eta_k E^k(q)_i, \quad (12)$$

with the quadratic approximation in the form of the inner product

$$V = \frac{1}{2} \langle q, (U - \eta_k E^k) q \rangle, \quad (13)$$

where the η_k ($k = 1, 2 \dots m$) are independent parameters, and U is the strain energy (symmetric and positive definite). In terms of the equations of motion we use Lagrange's equation to obtain

$$M\ddot{q} + (U - \eta_k E^k)q = 0, \quad (14)$$

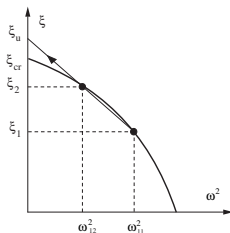
and assuming harmonic motion in the usual way, $q = ue^{\lambda t}$, we obtain the characteristic equation

$$|M\lambda^2 + U - \eta_k E^k| = 0. \quad (15)$$

For conservative systems we have $\lambda = i\omega$ with λ^2 identified as the negative of the square of the natural frequencies. We are, of course, primarily interested in systems for which $q = 0$ represents a stable system but may become unstable (at buckling), and this occurs when one of the eigenvalues vanishes. Although instability may occur via a complex pair of eigenvalues in non-conservative systems (flutter, e.g., [Beck's problem](#)) we are primarily focused on the conditions under which a real eigenvalue vanishes at the [divergence](#) boundary.

The relation between ω^2 and η_k constitutes the characteristic curve (or surface, when more than one parameter is present). It has been proven that for conservative systems with a trivial equilibrium state, any number of degrees of freedom, and equations of motion that are linear in the parameters η_k , the surface involving the fundamental frequency cannot have convexity toward the origin. Furthermore, it also follows that the fundamental surface is a plane (or straight line for a system with a single parameter) if the matrices M , U , and E^k can be reduced to a diagonal form simultaneously.

The divergence boundary is contained in the characteristic curve and obtained by setting $\omega^2 = 0$. If a single parameter ξ (load) is acting on the system, then it is possible to obtain an (upper bound) estimate of the critical value. From the figure below we see that if we know the frequencies at two values of the loading parameter ξ : $\omega_{11}^2(\xi_1)$ and $\omega_{12}^2(\xi_2)$ we can gain an estimate of frequencies at other loading values. Of course, if the characteristic curve is a straight line (e.g., if the equations uncouple) then this estimate will be exact. By extrapolating a line joining them we obtain an *upper bound* on the critical value of ξ from the intersection with the ξ -axis.



Convexity of the characteristic curve and its implication for providing a lower bound (Huseyin).

Snap-Through Revisited

In **snap-through buckling** we might still expect to monitor the lowest natural frequency to predict instability but the nonlinearity of the underlying equilibrium curve can also have an influence. We consider the dynamics of a system in the vicinity of a saddle-node bifurcation:

$$\ddot{X} - X^2 - \lambda = 0, \quad (16)$$

where both the deflection X and the load parameter λ are measured from the origin. Now suppose we have an equilibrium position (X_e) and we wish to study the behavior of small oscillations about it. We can expand equation (16) in the usual way by replacing X by $X_e + x$ which leads to

$$\ddot{x} - X_e^2 - 2X_e x - x^2 - \lambda = 0. \quad (17)$$

The x^2 term can be dropped because it is **small**, and due to equilibrium we also have $-X_e^2 - \lambda = 0$, and thus we are left with the linearized equation of motion

$$\ddot{x} - 2X_e x = 0. \quad (18)$$

This system has the natural frequency

$$\omega = \sqrt{-2X_e} = \sqrt{+2(-\lambda)^{1/2}}, \quad (19)$$

and thus, for large negative λ say, we observe a linear relation between the loading parameter and the **fourth** power of the natural frequency.

Effect of Damping

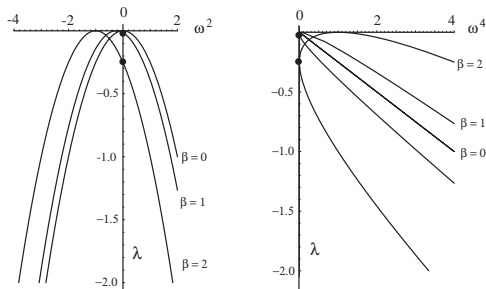
So far we have concentrated mainly on undamped systems. In most of the mechanical systems of interest there is usually a little energy dissipation and we shall assume that this takes the form of a **linear viscous damping**. Thus we consider

$$\ddot{X} + \beta\dot{X} - X^2 - \lambda = 0. \quad (20)$$

Conducting a similar analysis to the previous section we arrive at relationships between the natural frequency (the harmonic factor in the decaying, oscillating motion) and load parameter of

$$\begin{aligned} \omega^2 &= \pm 2(-\lambda)^{1/2} - (\beta/2)^2, \\ \omega^4 &= 4(-\lambda) \pm 4(-\lambda)^{1/2}(\beta/2)^2 + (\beta/2)^4. \end{aligned} \quad (21)$$

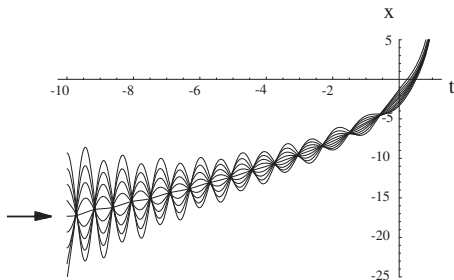
These expressions are plotted below for three values of damping including the undamped case.



The effect of damping on the frequency - load parameter relation.

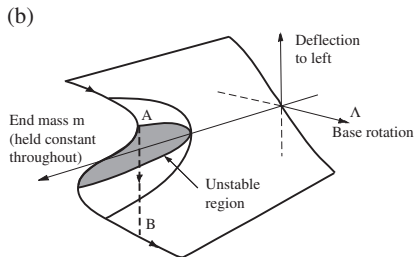
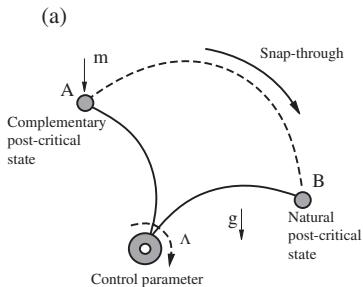
We see that damping has the effect of causing the natural frequency to diminish to zero **prior** to buckling. For example, with a damping level of $\beta = 2$ (and assuming the damping coefficient is constant) we observe that oscillations will cease when the load reaches a value of about $\lambda = -0.25$.

We can again integrate the equation of motion while slowly sweeping through the load parameter (as was done earlier). For example, the figure below shows nine trajectories generated for the system equation (20) and using a constant value of the **initial total energy** with $\beta = 0.5$, λ evolved at the rate $30t$, with the initial conditions prescribed by $\dot{x}(0) = 0.0$, $x(0) = -\sqrt{300} + A$, where A varied between -8 and 8 in increments of 2 .



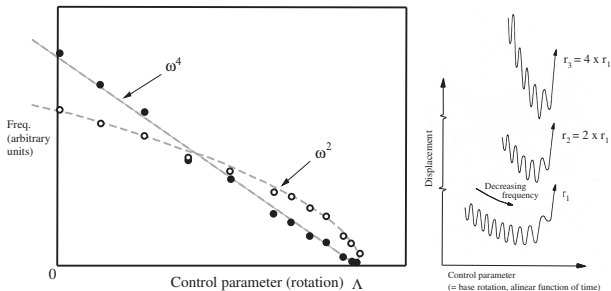
Some trajectories plotted as time series as the system is swept toward the saddle-node bifurcation.

A simple experimental verification of this situation is shown below. Here, a flexible rod with an end mass in a heavily postbuckled configuration was subject to base rotation such that a saddle-node bifurcation was encountered. The base rotation can be thought of as **control** in our standard system of gravity acting on the mass.



(a) A flexible strut with an end mass, (b) control surface showing a transition through bifurcation.

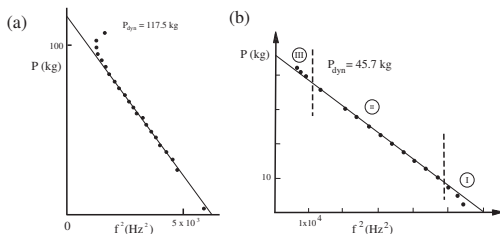
The measured frequencies and their relation to the control parameter are shown plotted below. Part (b) shows some time series in which the parameter r is a measure of the rate at which the base is rotated. We see that raising the frequency to the **fourth power** provides a more linear relationship than for the second power with which to predict **criticality**.



(a) Measured frequencies for the flexible strut rotated through a saddle-node bifurcation, (b) some sample time series with different rates of rotation.

Range of Prediction

We note that damping, changing boundary conditions, initial imperfections, type of instability, etc., all conspire to make predictions more difficult.



The load-frequency (squared) relation for (a) rectangular duraluminum plate, (b) laminated composite column. (Chailleux et al.)

Shown here are results from a laminated composite column in which the authors identified three distinct regions, with region II providing the most useful (linear) relation for prediction purposes. Also in part (b), the authors noted that with very low load levels they experienced some clearance in the boundary conditions.

Given that raising the frequency to either the second or fourth power might be a more appropriate predictor, it seems reasonable to raise the frequency to various powers in order to see how the subsequent curve might change from concave to convex, which then has clear implications for **lower bound estimates**. Plaut and Virgin studied the effect of extrapolating frequency raised to various power with a special reference for the range over which data were measured. That is, by raising the frequency to various powers a value is reached whereby the relation changes from convex to concave, with the transition point providing a close-to-linear relationship.

A Box Column

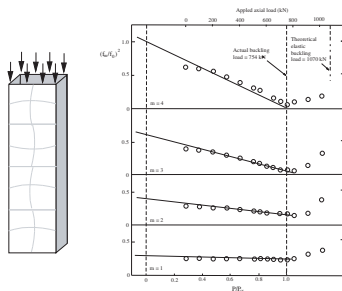
A notable piece of work on the dynamic non-destructive evaluation of structures was conducted by Jubb, Phillips and Becker. The authors conducted some tests on box columns, which provided a clever way of studying plates incorporating simply-supported edges. One of their main goals was to establish a means of assessing the effects of residual stresses on the stiffness, dynamics and stability of a typical structure. They suggested using the following variation on the frequency (f)-load (σ) theme

$$k \frac{\sigma_r}{\sigma_{cr}} + \frac{\sigma_a}{\sigma_{cr}} + \left(\frac{f}{f_0} \right)^2 = 1. \quad (22)$$

In this expression, the residual stress, σ_r , is added to the external stress, and k is a constant (less than unity) that takes account of stress distribution.

In the experiments of Jubb et al. they chose an aspect ratio of 4. In the absence of axial load, if the frequency corresponding to 4 half sine waves in the longitudinal direction ($m = 4$) is denoted by 1.0, the lower modes turn out to have relative frequencies of 0.610 ($m = 3$), 0.391 ($m = 2$) and 0.282 ($m = 1$). As the axial force increases, these frequencies decrease (linearly with frequency squared) but at **different rates** such that it is the $m = 4$ mode that drops to zero at buckling (i.e., $P/P_{cr} = 1$).

The experimental results are shown below.

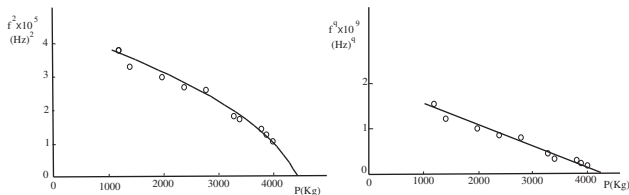


The four lowest frequencies for the box column plotted as a function of the applied axial load. Adapted from Jubb et al.

The welded corners induce a degree of **residual stress** such that the initiation of an applied axial load does not correspond to zero axial load in the frequency-load relation. Also, a degree of post-buckling stiffening is apparent in each of the modes. Therefore it may be important to monitor the first few lowest natural frequencies in order to capture the appropriate buckling mode.

Plates and Shells

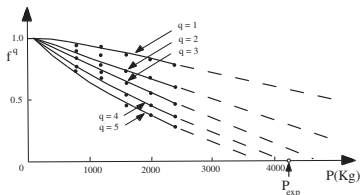
A thorough body of work on non-destructive testing of cylindrical shells under axial loading using dynamic (vibration) characteristics is due to Singer and his colleagues. An example of this type of research is shown below:



The lowest vibration frequency of an axially-loaded cylinder. (a) frequency squared, (b) frequency raised to the power $q = 2.9$. Adapted from Singer et al.

The cylinder included rib-stiffeners, which had the effect of reducing some of the imperfection-sensitivity typically encountered in axially-loaded shells. Part (a) shows a conventional frequency-squared versus load plot. Part (b) shows the same data with the frequency raised to the 2.9th power.

The figure shows a plot in which (lower load level) frequencies are raised to various powers and then extrapolated.



The same frequencies as in the previous slide but raised to various powers and subsequently extrapolated (linearly) to the buckling load. Adapted from Singer et al.